Conclusion: Mucoepidermoid carcinoma of the bronchus is often visualized as marked heterogeneous contrast enhancement on HRCT images. The results of this study suggest that the presence of abundant microvessels, detected immunohistochemically by microscopic examination, affects the enhancement pattern on HRCT.

1. Introduction

Mucoepidermoid carcinoma of the lung is an extremely rare tumour, comprising less than 5% of primary bronchial tumours and 0.1–0.2% of all lung cancers [1–4]. The largest series (56 cases over 26 years) has been published by Yousem and Hochholzer [3]. These tumours are thought to originate from bronchial gland of minor salivary gland-type lining the bronchi, and are classified into low grade and high grade on the basis of histological criteria [1,3,5]. The most important factors in the prognosis include the histological grade and whether complete surgical resection is possible. Completely resectable low-grade tumours generally have an excellent prognosis [3,6].

The radiological appearance of mucoepidermoid carcinoma of the lung depends on tumour location, size and whether obstructive pneumonia is present. The reported computed tomographic (CT) appearance of mucoepidermoid carcinoma of the lung is a well circumscribed oval or lobulated mass arising within the bronchus [7]. Although some investigators have reported the CT features of this tumour [7–10], few reports have included detailed findings of high-resolution CT (HRCT) or correlated them with histopathologic features. The purpose of this study was to characterize the HRCT findings of mucoepidermoid carcinoma of the lung and correlate them with the histopathologic features.

2. Materials and methods

The patients investigated in this study presented at the National Cancer Center, Tokyo, Japan, for diagnosis and treatment during the period from January 1999 through December 2005. Only patients with primary mucoepidermoid carcinoma of the lung were included; patients with pulmonary metastasis from remote sites were excluded. Five patients underwent HRCT and were treated for primary mucoepidermoid carcinoma. The diagnosis was confirmed by histopathologic examination of the surgical specimen in all five patients. All clinical records, including the follow-up information, HRCT findings, endoscopic images and gross and microscopic specimens, were reviewed retrospectively.

2.1. HRCT protocols

HRCT was performed with either a 4-row or 16-row multi-detector CT (MDCT) scanner (Aquilion V-detector, Toshiba Medical Systems Corp., Tokyo Japan). The patients were evaluated with the MDCT scanner by using axial 2.0 mm × 4 mm or 16 modes, 120 kVp, 200–250 mA, and thin-section CT images were obtained using 1.0 mm sections reconstructed at 2.0 mm intervals with a high-spatial-frequency algorithm and retrospectively retargeted to each lung with a 20 cm field of view (FOV). All patients were intravenously injected with 80–150 ml of non-ionic contrast medium at a rate of 2.0–3.0 ml/s with an autoinjector (Autoenhance A-250, Nemoto Kyorindo, Tokyo, Japan), and scanning was started after a 40 s delay. Hard-copy images were photographed at window settings for the lung (center, −600 HU; width, 2000 HU) and the mediastinum (center, 35 HU; width, 400 HU). The intervals between the CT examinations and surgery ranged from 2 days to 4 weeks. All patients were followed up regularly in our institute. Follow-up CT images were obtained in all patients.

The HRCT images were assessed by two independent observers without reference to the clinical findings. The location of the pulmonary nodule was classified as peripheral or central. Nodules present within the peripheral two-thirds of the lung were arbitrarily classified as peripheral type and those within the central one-third or in contact with lobar or segmental bronchi were classified as central. The CT analysis included determination of the attenuation coefficient of the pulmonary lesion. CT attenuation coefficient was evaluated before and after administration of contrast media. The contrast enhancement of the tumour was compared with that of the chest wall musculature. Whether intratumoral calcification was present was also noted. After making independent initial evaluations, the two observers reviewed all cases in which their interpretations differed and reached a final consensus.

2.2. Histopathologic examination

Surgical specimens were inflated and fixed by transpleural and transbronchial infusion with formalin. The specimens were sectioned transversely in the same planes as the HRCT images, stained with hematoxylin-eosin and immunostained for the endothelial marker CD31. One of the authors, an experienced pulmonary pathologist, reviewed the histopathologic findings. The characteristics of the tumours on the HRCT images were compared with the histopathologic findings.

3. Results

3.1. Clinical features

The clinical data are summarized in Table 1. The five patients (two males and three females) ranged in age from 22 to 58 years, and their average age was 41.6 years. Only two of them were smokers. Four of the patients complained of chronic symptoms, including cough, increased sputum production and episodic fevers. These symptoms were related to bronchial irritation, partial or complete bronchial obstruction and distal pneumonia. The remain-

Table 1 Clinical data of patients with mucoepidermoid carcinoma of the bronchus

Case	Age (year)	Sex	Symptom	Tumour location	Tumour site	Preoperative diagnosis
1	22	M	Cough, sputum	Central	Lt. LLB (B6)	Mucoepidermoid Ca.
2	40	W	Fever, chest pain	Central	Rt. MLB	Mucoepidermoid Ca.
3	58	W	Cough, sputum, fever	Central	Rt. BB (B9)	Non-typed malignant tumour
4	51	M	None	Peripheral	Rt. MLB (B4a)	No malignancy
5	37	W	Cough, sputum, fever	Central	Lt. UDB	No biopsy

Lt. LLB, Left lower lobe bronchus; Rt. BB, right basal bronchus; Rt. MLB, right middle lobe bronchus; Lt. UDB, left upper division bronchus.

ing patient was asymptomatic, and the lesion was detected during routine health examination.

The serum sialyl Lewis X-i antigen (SLX) values were high in all five cases. The serum carcinoembryonic antigen (CEA) and carbohydrate antigen 19-9 (CA19-9) values were high in three cases. The serum cytokeratin fragment 19 (CYFRA 21-1), squamous cell carcinoma antigen (SCC), neuron specific enolase (NSE), progastrin-releasing peptide (pro-GRP) values were all within the normal range.

3.2. HRCT findings

On the CT images, the tumours ranged in diameter from 18 to 38 mm (mean, 28.4 mm) (Table 2). The lesions were located in the central lung in four cases and in the peripheral lung in one. All the lesions were well defined nodules or masses with a smooth margin (Fig. 1). The contour of the tumours was round ($n=1$), oval ($n=3$) or lobulated ($n=1$). Non-enhanced CT scans revealed intratumoral punctate calcification in one of the five lesions (Case 1). CT findings suggestive of bronchial stenosis or obstruction were seen in all cases (distal obstructive pneumonia in four cases, distal bronchial dilation in four and atelectasis in three). Atelectasis with recurrent or non-resolving pneumonia was observed distal to the site of obstruction.

CT attenuation coefficients were evaluated before and after administration of contrast medium. Thus, the change of CT attenuation or the degree of contrast enhancement was described. CT images enhanced by intravenous contrast medium showed marked heterogeneous enhancement with foci of relatively low attenuation in four of the five lesions and mild heterogeneous enhancement in the other lesion. Measurement of Hounsfield unit (HU) data was possible in every patient. The attenuation coefficients of the four markedly enhanced tumours (range, 95–139 HU; mean, 118.5 HU) were much higher than those of the chest wall musculature (range, 48–68; mean, 61.3 HU), whereas that of the one mildly enhanced tumour was slightly higher than that of the chest wall musculature. The ratio of the attenuation coefficient of the tumour to that of the musculature in the mildly enhanced case was 1.5, whereas those of the markedly enhanced cases were much higher (range, 2.0–2.2) (Table 2). None of the patients had lymphadenopathy in the mediastinum, pulmonary hilum or around the bronchi, on the basis of the CT findings.

3.3. Bronchoscopic findings

Bronchoscopy was performed in all five cases and the tumours were easily visualized except the peripheral lesion. The tumours were located in the lobar or segmental bronchi and had filled the bronchial lumen. They were soft, polypoid with a sessile base and pink like the bronchial mucosa. Three of the tumours were covered by a highly vascular mucosa. Although bronchoscopic brushing or biopsy was performed in four cases, a preoperative diagnosis of mucoepidermoid carcinoma was made in only two of them. Bronchoscopy in the other two cases revealed a non-typed malignant tumour or non-diagnostic inflammatory cells.

3.4. Treatment

The treatment chosen for all patients was surgical resection, and the procedure consisted of routine lobectomy including right middle and lower lobectomy (Table 2). The surgical procedures resulted in tumour-free margins. Lymph node dissection or sampling of pulmonary hilar and mediastinal lymph nodes was performed in all cases.

3.5. Histopathologic findings

The histologic diagnosis was low-grade mucoepidermoid carcinoma in all five cases (Table 3). The central tumours

Table 2 HRCT findings of mucoepidermoid carcinoma of the bronchus in four patients

Case	Tumour size (mm)	Tumour margin	Tumour contour	Pattern of enhancement	Ratio of attenuation coefficient
1	38 × 35	Well defined (smooth)	Oval	Heterogeneous	2.1
2	26 × 18	Well defined (smooth)	Lobulated	Heterogeneous	1.5
3	34 × 22	Well defined (smooth)	Oval	Heterogeneous	2.1
4	24 × 24	Well defined (smooth)	Round	Heterogeneous	2
5	33 × 29	Well defined (smooth)	Oval	Heterogeneous	2.2

Ratio of attenuation coefficient: Ratio of the attenuation coefficient of the tumour to attenuation coefficient of the musculature

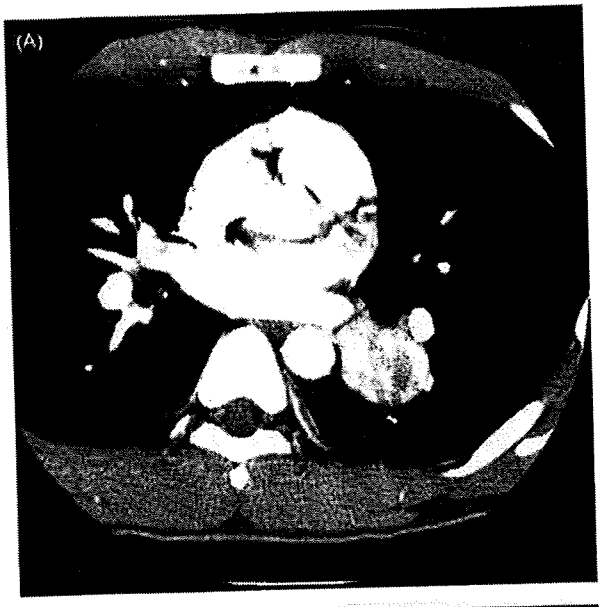

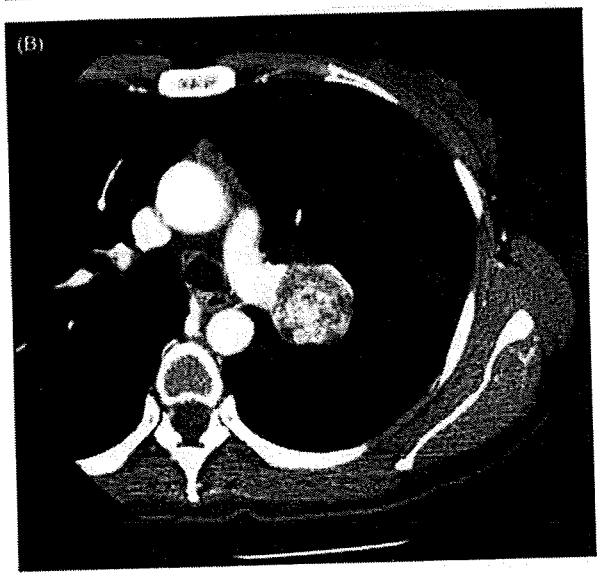

Fig. 1 Mucoepidermoid carcinomas of the bronchus were well defined mass and had a smooth margin. Enhanced CT images shows marked heterogeneous enhancement with foci of relatively low attenuation (A, Case 1; B, Case 5).

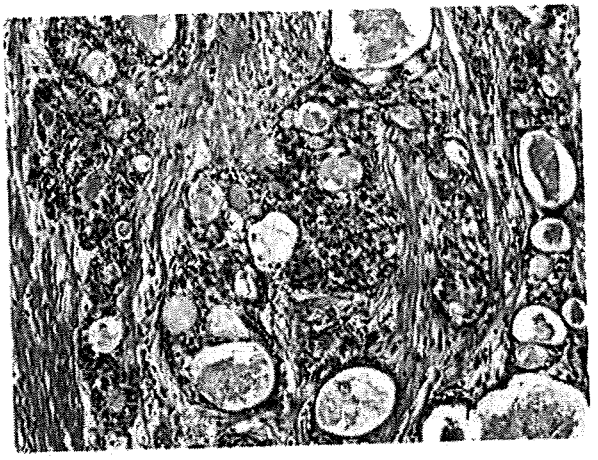

Fig. 2 High-magnification photomicrograph showed the epithelial component of the tumours consisted of mucin-secreting cells, squamoid cells and intermediate-type cells that displayed no specific differentiation.

protruded into the lumen of the bronchus and almost totally occluded it. On cut sections, the tumours were light yellow or tan polypoid masses. The margins and contours of the tumours were smooth, and they were well circumscribed and oval or round, consistent with their CT appearance.

Microscopically, the tumours were seen to arise from bronchial glands and to have infiltrated the bronchial wall. The epithelial component of the tumours consisted of mucin-secreting cells, squamoid cells and intermediate-type cells that displayed no specific differentiation (Fig. 2). Cystic change predominated in some areas, and the solid areas comprised mucin-secreting columnar epithelium that had formed small glands, tubules and cysts. There were no prominent nucleoli, and mitotic figures and necrosis were absent or minimal (less than five mitoses per 50 high-power fields). Keratinization was rare or absent in the epidermoid areas. These pathologic findings are characteristic of low-grade mucoepidermoid carcinoma. There was an admixed distribution of areas that are heterogeneous in the densities of blood vessels, as highlighted by immunohistochemical staining of CD31. Most mucin-secreting areas of the tumours showed more densely distributed blood vessels, mostly capillaries, in between tumour cell nests, whereas other areas did less (Fig. 3). Stromal calcification and ossification with a granulomatous reaction was observed in Case 1. The histologic specimens in Case 1, in which intratumoral punctate calcifications were observed on non-enhanced HRCT scans, showed microscopic calcification. Distal obstructive pneu-

Table 3 Histopathologic findings and outcome

Case	Treatment	p-Stage (TNM)	Grade	CD31	Outcome
1	Left lower lobectomy	T2N0M0 IB	Low-grade	(++)	NED
2	Right middle and lower lobectomy	T1N0M0 IA	Low-grade	(++)	NED
3	Right lower lobectomy	T2N0M0 IB	Low-grade	(+)	NED
4	Right middle lobectomy	T1N0M0 IA	Low-grade	(++)	NED
5	Light upper lobectomy	T2N0M0 IB	Low-grade	(++)	NED

NED: No evidence of disease.

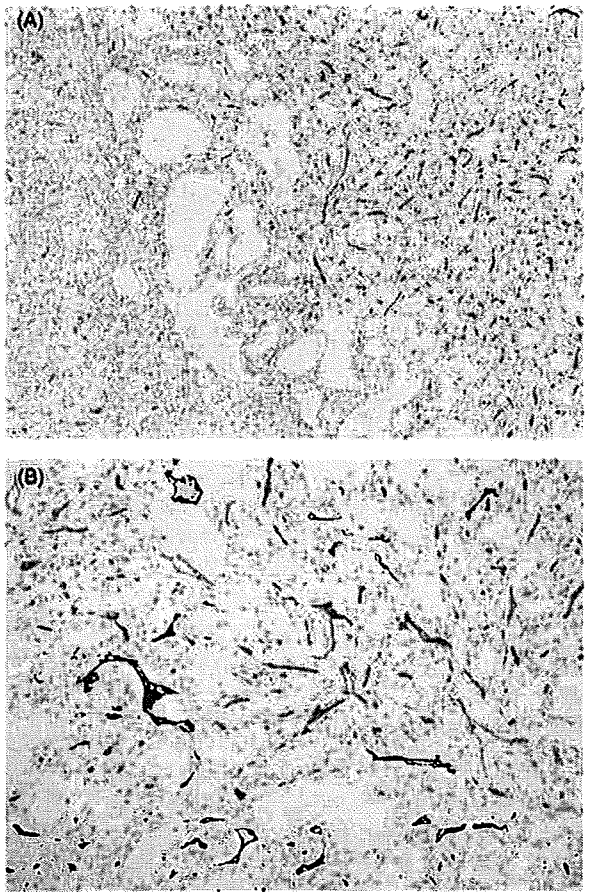

Fig. 3 (A) Immunohistochemical findings showing a border of areas with and without dense blood vessels as highlighted by anti-CD31 antibody. Note the abundant glands with mucus production in the right half, where there are more vessels labeled by anti-CD31 antibody. (B) Higher magnification of the area with plenty of mucin-secreting glands. Immunoreactive CD31 label the surface of endothelial cells, but not mucin of the tumour.

monia was observed in four patients with lesions of the central type, and distal bronchial dilation and mucoid impaction was seen in all five cases. The secondary findings associated with bronchial stenosis or obstruction on the HRCT scans largely reflected these pathologic findings. No lymph node metastasis was found in any of the surgical specimens.

4. Discussion

Mucoepidermoid carcinoma of the lung was first reported by Smetana et al. [11], and accounts for only a very small proportion of primary lung cancers. The tumours are classified as low grade or high grade based on their histologic appearance, and grading is based on cellular atypia, mitotic activity, local extension and tumour necrosis. Low-grade mucoepidermoid carcinoma is the most common type, and all five of the tumours in our series were low-grade. Although there is good clinicopathological evidence for the existence of the low-grade type, it has been questioned whether the high-grade type is a separate entity, mainly because of its histological similarity to mixed pulmonary carcinomas [5]. The high-grade variant is occasionally difficult to differentiate from adenosquamous carcinoma [12–14].

The most common symptoms are related to intraluminal growth, and these include persistent cough and sputum, wheezing, dyspnea, recurrent pneumonia, and, less frequently, hemoptysis [15]. Since the symptoms do not differ from those of other forms of lung tumour, they do not contribute to the differential diagnosis. Most patients with mucoepidermoid carcinoma are misdiagnosed as having bronchitis or lung carcinomas of other types. In our series, one patient was asymptomatic and the others had such similar symptoms that they were initially misdiagnosed as having chronic obstructive airway disease or other airway tumours.

Although the central-type tumours in our series were readily visible, only two of them were diagnosed preoperatively as mucoepidermoid carcinoma. Since mucoepidermoid carcinomas of the bronchi are usually covered by normal respiratory mucosa, bronchial brushing and lavage are seldom diagnostic, and it is better to perform a biopsy with forceps. Despite the theoretical risk of severe hemorrhage by performing a biopsy on a vascular mass, hemorrhage has never been reported as a complication of biopsy for mucoepidermoid carcinoma of the bronchus. Nevertheless, care is required because of the highly vascular nature of many of the tumours.

CT scan is non-invasive and useful for evaluating suspected endobronchial lesions, and fine morphological features have been revealed since the introduction of HRCT. In this series, HRCT images were essential for identifying the more detailed characteristics of the tumours, such as the margin, shape, density and pattern of enhancement. For the most part, the HRCT images reflected the pathologic features of the tumours well. There have been a few case reports of the HRCT appearance of mucoepidermoid carcinoma of the lung [7,10]. The HRCT features of the tumours in our series, such as a smooth margin and a well defined oval or round shape, were similar to those reported by Kim et al., who also found intratumoral punctate calcification on non-enhanced CT scans. Secondary findings associated with bronchial stenosis or obstruction, such as distal obstructive pneumonia, bronchial dilatation and atelectasis, were also seen. Although in their series Kim et al. reported mucoepidermoid carcinoma of the bronchus as showing mild contrast enhancement on CT scans, the three lesions of the central type and one lesion of the peripheral type in our series demonstrated marked contrast enhancement on HRCT images. The attenuation coefficients of the markedly enhanced tumours were much higher than those of the chest wall musculature.

Immunohistochemical staining for CD31 highlighted the heterogeneous distribution of blood vessels from mucin-secreting areas to non-secreting areas in a single tumour. In other words, these lesions may have characteristics of both hypervascular and hypovascular components, and the presence of both was probably the explanation for the features we observed on HRCT. The results of this study suggested that the presence of abundant microvessels, detected immunohistochemically by microscopic examination, affected the enhancement pattern on HRCT. These histopathologic findings correlated with the HRCT findings in all patients.

Bronchogenic carcinomas with more common histologic features, including adenocarcinoma, squamous cell carcinoma and small cell carcinoma have a variety of radiologic manifestations. Adenocarcinoma is often distinct from the other histologic subtypes of lung cancer. Non-solid nodules (ground glass opacities) and partly solid nodules (mixed solid/ground glass opacities) are recognized patterns of adenocarcinoma. Henschke et al. reported that the malignancies in subsolid nodules were typically bronchioloalveolar carcinomas or adenocarcinomas with bronchioloalveolar features, whereas in solid ones the malignancies were typically other subtypes of adenocarcinoma [16]. The proportion occupied by the non-solid component based on volumetric analysis by CT scan is a reliable predictor of tumours without vessel invasion in patients with adenocarcinoma of the lung [17]. Central squamous cell carcinoma is characterized by two major patterns of spread: intraepithelial spread with or without subepithelial invasion, and endobronchial polypoid growth. Polypoid tumours often occlude the bronchial lumen, resulting in atelectasis and obstructive pneumonia. Peripheral squamous cell carcinomas are seen as solid nodules, occasionally with cavitation and irregular margins. Approximately 90–95% of all small cell lung cancers are located centrally and show mediastinal or hilar lymphadenopathy with displacement or narrowing of the tracheobronchial tree or major vessels [18]. These common histologic types of lung cancer usually show mild or less contrast enhancement on CT images. Since these CT findings in common forms of lung carcinoma differ from those of mucoepidermoid carcinoma, which are relatively characteristic, contrast-enhanced CT may be helpful for lesion characterization and tumour classification in affected patients. If a marked heterogeneous contrast enhancement pattern is observed in well circumscribed oval or round masses of the bronchus, mucoepidermoid carcinoma can be considered in the differential diagnosis.

Large cell neuroendocrine carcinoma shows non-specific CT findings similar to those of other non-small cell lung cancer. On contrast-enhanced CT scans, tumour attenuation varies from slightly less to more than that of the chest wall muscle, with a homogeneous or heterogeneous pattern [18,19]. However, large cell neuroendocrine carcinoma is more likely to appear in the peripheral lung. Adenosquamous carcinoma of the peripheral type also usually shows heterogeneous soft-tissue attenuation [20]. Histopathologically, adenosquamous carcinoma is occasionally difficult to differentiate from high-grade mucoepidermoid carcinoma, which invades the pulmonary parenchyma in nearly 46% of the cases [3,12–14].

Pulmonary carcinoid tumours, which are low-grade malignancies accounting for 2–3% of all lung neoplasms [21], show CT findings similar to those of mucoepidermoid carcinoma. Pulmonary carcinoid tumours are also known to be vascular, and often show marked contrast enhancement on CT images [18,22]. Therefore, it is difficult to differentiate pulmonary carcinoid tumour from mucoepidermoid carcinoma on the basis of the CT contrast enhancement pattern alone.

Follow-up information was available for all five of the present cases. The clinical course of the patients was correlated with the histologic grade of their tumours. Low-grade mucoepidermoid carcinoma generally grows locally and is amenable to complete surgical resection. Low-grade tumours spread to regional lymph nodes by local growth in less than 5% of cases, and distant spread is rare [3,15]. The prognosis of low-grade tumours is usually excellent, with no evidence of local recurrence or metastasis. However, Barsky et al. [23] reported cases that were diagnosed as well differentiated and low-grade malignancy histologically but were rated as high-grade malignancy clinically. It can therefore be concluded that the histologic malignancy level of the tumour is not always the same as its clinical malignancy level. This suggests that complete surgical resection plus lymph node dissection should be performed for low-grade mucoepidermoid carcinoma of the bronchus as well as high-grade mucoepidermoid carcinoma. All five patients in our series underwent lobectomy plus lymph node dissection or sampling, and all are currently alive without evidence of disease at an average of 50.4 months after surgery (range, 15–82 months; median, 57 months).

5. Conclusions

We reviewed the HRCT and pathologic findings in five cases of mucoepidermoid carcinoma of the lung. Mucoepidermoid carcinoma is often visualized as marked heterogeneous contrast enhancement on HRCT images. The presence of abundant microvessels, detected immunohistochemically by microscopic examination, may affect the enhancement pattern on HRCT. However, examinations of HRCT images of mucoepidermoid carcinoma of the lung are insufficient because of the rarity of the tumour. The HRCT characteristics of the tumour must therefore be evaluated in more cases.

Conflict of interest

None declared.

References

[1] Colby TV, Koss MN, Travis WD. Tumors of salivary gland type. Tumors of the lower respiratory tract: AFIP atlas of tumor pathology 3rd series, vol. 13. Washington, DC: American Registry of Pathology; 1995. p. 65–89.
[2] Spencer H. Bronchial mucous gland tumours. Virchows Arch A Pathol Pathol Anat 1979;383:101–15.
[3] Yousem SA, Hochholzer L. Mucoepidermoid tumors of the lung. Cancer 1987;60:1346–52.
[4] Miller DL, Allen MS. Rare pulmonary neoplasms. Mayo Clin Proc 1993;68:492–8.
[5] Klacsmann PG, Olson JL, Eggleston JC. Mucoepidermoid carcinoma of the bronchus: an electron microscopic study of the low grade and the high grade variants. Cancer 1979;43: 1720–33.
[6] Heitmiller RF, Mathisen DJ, Ferry JA, Mark EJ, Grillo HC. Mucoepidermoid lung tumors. Ann Thorac Surg 1989;47: 394–9.
[7] Kim TS, Lee KS, Han J, Im JG, Seo JB, Kim JS, et al. Mucoepidermoid carcinoma of the tracheo-bronchial tree: radiographic and CT findings in 12 patients. Radiology 1999;212:643–8.
[8] Fisher DA, Mond DJ, Fuchs A, Khan A. Mucoepidermoid tumor of the lung: CT appearance. Comput Med Imaging Graph 1995;19:339–42.

[9] Tsuchiya H, Nagashima K, Ohashi S, Takase Y. Childhood bronchial mucoepidermoid tumors. J Pediatr Surg 1997;32:106–9.
[10] Kinoshita H, Shimotake T, Furukawa T, Deguchi E, Iwai N. Mucoepidermal carcinoma of the lung detected by positron emission tomography in a 5-year-old girl. J Pediatr Surg 2005;40:E1–3.
[11] Smetana HF, Iverson L, Swan LL. Bronchogenic carcinoma. Analysis of 100 autopsy cases. Milit Surg 1952;3:335–51.
[12] Leonardi HK, Jung-Legg Y, Legg MA, Neptune WB. Tracheobronchial mucoepidermoid carcinoma: clinicopathological features and results of treatment. J Thorac Cardiovasc Surg 1978;76:431–8.
[13] Stafford JR, Pollock J, Wenzel BC. Oncocytic mucoepidermoid tumor of the bronchus. Cancer 1984;54:94–9.
[14] Stafford JR, Pollock J, Wenzel BC. Bronchial mucoepidermoid carcinoma metastatic to skin. Report of a case and review of the literature. Cancer 1986;58:2556–9.
[15] Granata C, Battistini E, Toma P, Balducci T, Mattioli G, Fregonese B, et al. Mucoepidermoid carcinoma of the bronchus. Paediatr Pulmonol 1997;23:226–32.
[16] Henschke CI, Yankelevitz DF, Mirtcheva R, McGuinness G, McCauley D, Miettinen OS, et al. CT screening for lung cancer: frequency and significance of part-solid and nonsolid nodules. AJR Am J Roentgenol 2002;178:1053–7.
[17] Tateishi U, Uno H, Yonemori K, Satake M, Takeuchi M, Arai Y. Prediction of lung adenocarcinoma without vessel invasion: a CT scan volumetric analysis. Chest 2005;128:3276–83.
[18] Chong S, Lee KS, Chung MJ, Han J, Kwon OJ, Kim TS. Neuroendocrine tumors of the lung: clinical, pathologic, and imaging findings. Radiographics 2006;26:41–57.
[19] Oshiro Y, Kusumoto M, Matsuno Y, Asamura H, Tsuchiya R, Terasaki H, et al. CT findings of surgically resected large cell neuroendocrine carcinoma of the lung in 38 patients. AJR Am J Roentgenol 2004;182:87–91.
[20] Yu JQ, Yang ZG, Austin JH, Guo YK, Zhang SF. Adenosquamous carcinoma of the lung: CT-pathological correlation. Clin Radiol 2005;60:364–9.
[21] Davila DG, Dunn WF, Tazelaar HD, Pairolero PC. Bronchial carcinoid tumors. Mayo Clin Proc 1993;68:795–803.
[22] Fauroux B, Aynie V, Larroquet M, Boccon-Gibod L, Ducou le Pointe H, Tamalet A, et al. Carcinoid and mucoepidermoid bronchial tumours in children. Eur J Pediatr 2005;164:748–52.
[23] Barsky SH, Martin SE, Matthews M, Gazdar A, Costa JC. "Low grade" mucoepidermoid carcinoma of the bronchus with "high grade" biological behavior. Cancer 1983;51:1505–9.

Ann Nucl Med (2007) 21:299–302
DOI 10.1007/s12149-007-0018-y

CASE REPORT

F-18 FDG PET/CT imaging of low-grade mucoepidermoid carcinoma of the bronchus

Taichiro Ishizumi · Ukihide Tateishi
Shun-ichi Watanabe · Tetsuo Maeda · Yasuaki Arai

Received: 14 November 2006 / Accepted: 19 February 2007

Abstract Mucoepidermoid carcinomas in the bronchial tree are extremely rare tumors. Such tumors are classified into low-grade and high-grade on the basis of histological criteria. Fluorine-18-fluorodeoxyglucose positron emission tomography (F-18 FDG PET) is a useful technique for the evaluation of pulmonary lesions; however, to our knowledge, F-18 FDG PET findings in mucoepidermoid carcinoma of the bronchus have been described in only a few cases. Identifiable focal F-18 FDG uptake has been reported in high-grade mucoepidermoid carcinoma, but it is unclear whether F-18 FDG accumulates in low-grade mucoepidermoid carcinoma. Here, we present the case of a 37-year-old woman, with pathologically proven low-grade mucoepidermoid carcinoma, who underwent high-resolution computed tomography (CT) and F-18 FDG PET/CT before treatment.

Keywords Mucoepidermoid carcinoma · Low-grade tumor · F-18 FDG PET/CT · Lung

Introduction

Mucoepidermoid carcinoma of the bronchus is a very uncommon tumor, comprising only 0.1%–0.2% of primary lung cancers [1]. The tumor has been reported in patients ranging in age from 3 months to 78 years, but almost half of the reported cases have been in patients younger than 30 years [2–4]. The tumor is thought to originate from the minor salivary glands lining the bronchi [4], and is classified as low-grade or high-grade on the basis of histological criteria [1, 4, 5].

Fluorine-18 fluorodeoxyglucose (F-18 FDG) positron emission tomography (PET) is increasingly used in the diagnostic workup of pulmonary lesions that are suspected to be malignant tumors. However, there are only a few reports of F-18 FDG PET findings in mucoepidermoid carcinoma of the bronchus [6, 7]. Here, we describe F-18 FDG PET/computed tomography (CT) imaging in a case of low-grade mucoepidermoid carcinoma of the bronchus.

Case report

A 37-year-old woman with no significant past history was referred to our hospital for the examination and treatment of an abnormal shadow on a chest roentgenogram. The patient had noted occasional blood-tinged sputum, cough, and episodic fevers for 6 months prior to admission. A chest roentgenogram revealed a left hilar mass (Fig. 1). Laboratory data showed an elevated serum sialyl Lewis X-i antigen (SLX) level (74 U/ml). Radiologic evaluation with a high-resolution CT (HRCT) scan showed a well-defined mass with a smooth margin. The contour of the tumor was oval. Intratumoral calcification was unclear on a non-enhanced CT scan, but an enhanced HRCT image showed marked heterogeneous enhancement with foci of relatively low attenuation (Fig. 2).

The lesion was thought to be a carcinoid or benign tumor, but its exact nature could not be determined from

T. Ishizumi (✉) · U. Tateishi · T. Maeda · Y. Arai
Divisions of Diagnostic Radiology and Nuclear Medicine, National Cancer Center Hospital, 5-1-1, Tsukiji, Chuo-Ku, 104-0045 Tokyo, Japan
e-mail: tishizumi@hotmail.co.jp

T. Ishizumi · S. Watanabe
Divisions of Thoracic Surgery, National Cancer Center Hospital, Tokyo, Japan

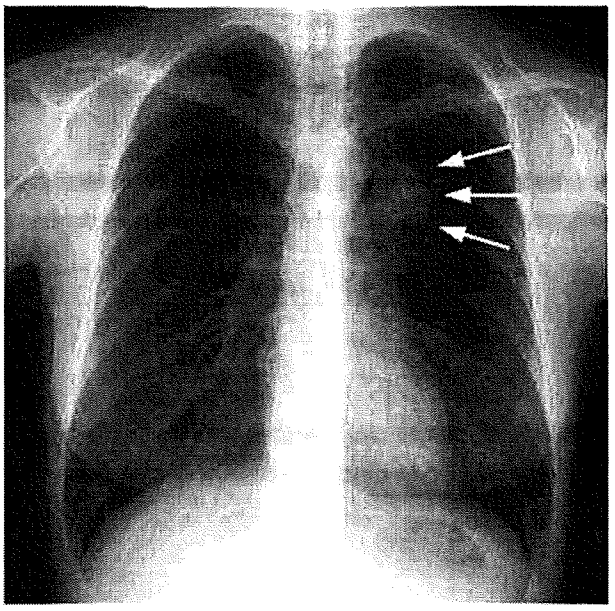

Fig. 1 Posteroanterior chest radiograph shows a well-defined mass adjacent to the left hilum (*arrow*)

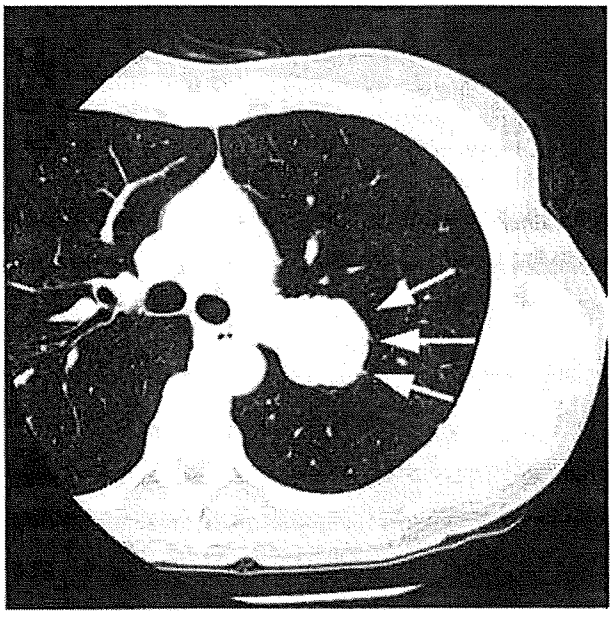

Fig. 2 High-resolution computed tomography (HRCT) findings of the left hilar lesion (*arrow*). A lobulated, heterogeneous mass is seen adjacent to the pulmonary artery

the CT scans. Therefore, FDG PET imaging was requested to allow differentiation of benign and malignant tumor and to evaluate the clinical stage. F-18 FDG PET/CT was performed with a PET/CT scanner (Biograph; Siemens/CTIMI, Knoxville, TN, USA). The transverse field of view (FOV) was 16.2 cm, and 47 image planes were produced. To correct for photon attenuation, a transmission CT scan was obtained prior to the emission scan. CT scanning was performed using a 16-detector row CT scanner (Toshiba Medical Systems, Tokyo, Japan). CT images were obtained using the following scan parameters: 120 kVp, 200–250 mA/rotation, 30–40 cm of FOV and a 512 × 512 matrix. The subjects were examined while in a supine position, and none received a contrast material. All images were obtained with the subject in deep inspiration. The patient fasted for at least 6 h before the PET/CT study and was tested to ensure a normal glucose level (range 4.9–6.7 mmol/l) before the PET scanning. An emission scan from the base of the skull to the mid-thigh was obtained starting 60 min after an intravenous injection of 296 MBq of F-18 FDG. The resulting F-18 FDG PET/CT fused images localized the abnormal uptake to the bronchial lesion (Fig. 3). The maximal standardized uptake value (SUV) of the tumor was 3.63, and there was no abnormal F-18 FDG uptake in the mediastinum.

Bronchoscopy was performed preoperatively. The tumor was easily visualized and was found to have filled the bronchial lumen. However, bronchoscopic biopsy was not performed because the tumor was covered with a highly vascular mucosa. The patient underwent left upper lobectomy with lymphadenectomy and pulmonary artery plasty. The pathological diagnosis was low-grade mucoepidermoid carcinoma of the bronchus. The surgical margins were all negative for tumor invasion, and there was no evidence of microscopic metastasis in the regional bronchopulmonary lymph nodes. Postoperatively, the patient has been healthy with no evidence of local or extrathoracic recurrence.

Discussion

The dissemination of F-18 FDG PET technology has enabled a functional approach to the evaluation of a pulmonary lesion that complements the anatomic assessment provided by chest radiography and CT scanning. Pulmonary lesions are difficult to diagnose accurately due to the limited sensitivity of non-invasive imaging, technical limitations of biopsy, and the high frequency of benign lesions. However, F-18 FDG PET is generally considered to have excellent sensitivity for the determination of malignancy in a pulmonary nodule [8, 9]; for example, Gould et al. found a sensitivity of 96.8% in a meta-analysis of the accuracy of F-18 FDG PET in the diagnosis of pulmonary nodules of 1 cm or more in diameter.

Low-grade malignant tumors of the lung, such as bronchioloalveolar carcinoma and carcinoid tumor, are

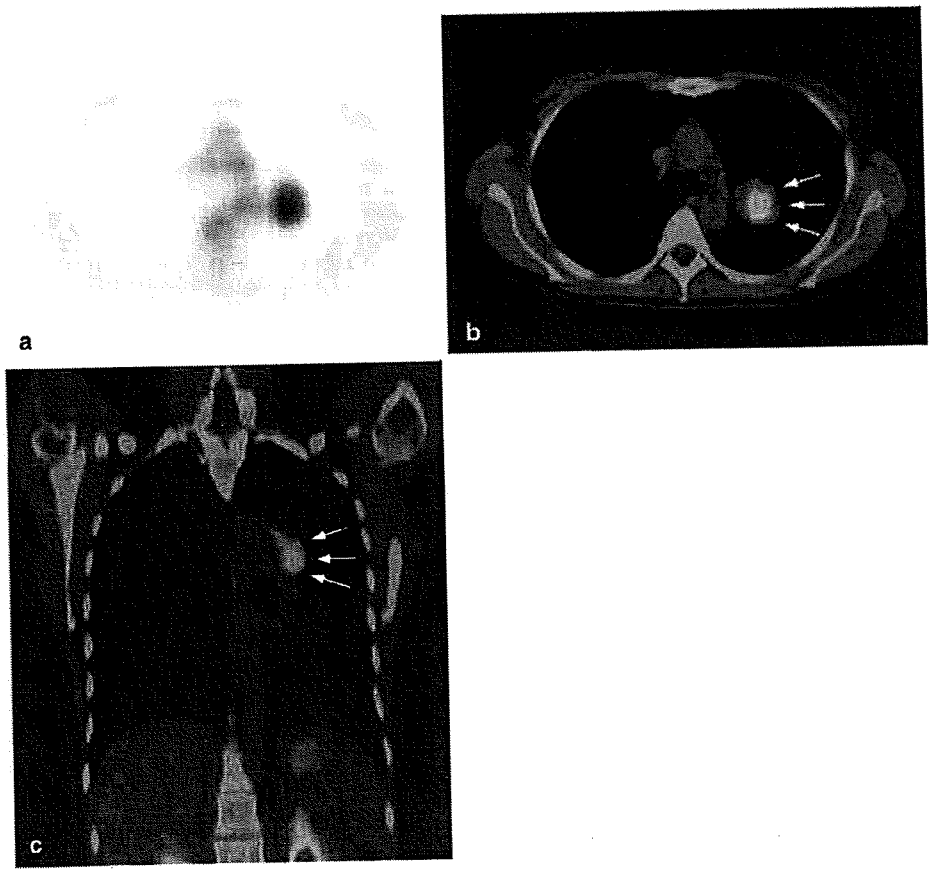

Fig. 3 Axial Fluorine-18-fluorodeoxyglucose positron emission tomography (F-18 FDG PET image) (**a**) shows a hypermetabolic area in the left lung. Axial (**b**) and coronal (**c**) fused images of PET/CT show a single focus of abnormal F-18 FDG uptake in the tumors (*arrow*). The maximal standardized uptake value (*SUV*) of the tumor was 3.63

typically negative in F-18 FDG PET imaging, and even if such tumors are positive they usually have lower F-18 FDG uptake than that expected for high-grade malignancies [10–12]. For example, Erasmus et al. reported that pulmonary carcinoid tumors of low-grade malignancy have lower F-18 FDG uptake than malignant tumors: 86% of the examined carcinoid tumors were found to be hypometabolic with an SUV < 2.5 [10]. Kruger et al. found that the SUV is <2.5 in half of pulmonary carcinoid tumors and recommended surgical resection or at least biopsy for solitary pulmonary nodules that are clinically suspected of being carcinoid, even if they are not hypermetabolic on F-18 FDG PET images [13]. However, even typical carcinoid tumors can show intense FDG uptake [14–16], and Daniels et al. have suggested that the overall PET sensitivity for detection of carcinoid tumors is 75%.

Few reports have described F-18 FDG PET findings in low-grade mucoepidermoid carcinoma of the lung. Focal F-18 FDG uptake has been reported in high-grade mucoepidermoid carcinoma [7], but the extent of F-18 FDG accumulation in low-grade mucoepidermoid carcinoma is unknown. In the present case, the patient underwent F-18 FDG PET/CT scanning preoperatively because the nature of the lesion could not be defined by HRCT imaging. The F-18 FDG PET/CT image of the tumor showed abnormal FDG uptake and the maximal SUV of the tumor was 3.63. This result suggests that the tumor had mild accumulation of FDG for the size of the lesion. Therefore, we first suspected the pulmonary lesion to be a benign or low-grade malignant tumor, such as a carcinoid tumor, based on HRCT and F-18 FDG PET imaging. Hence, if mild accumulation of F-18 FDG for tumor size is observed in a well-defined tumor with a smooth margin, we suggest that mucoepidermoid carcinoma should be considered as a differential diagnosis. However, examinations of F-18 FDG PET/CT images of mucoepidermoid carcinoma of the bronchus are insufficient because of the rarity of the tumor. The F-18 FDG PET/CT characteristics of the tumor must therefore be evaluated in more cases.

Conclusions

We demonstrated F-18 FDG PET/CT images of low-grade mucoepidermoid carcinoma of the bronchus. The F-18 FDG PET/CT image of the tumor in this case

showed abnormal F-18 FDG uptake. If mild accumulation of F-18 FDG for tumor size is observed in a well-defined tumor with a smooth margin, mucoepidermoid carcinoma should be considered as a differential diagnosis.

Acknowledgments The authors are indebted to H. Kato of Tokyo Medical University for his review of the manuscript. This work was supported in part by grants from Scientific Research Expenses for Health and Welfare Programs, No. 17–12, the promotion and standardization of diagnostic accuracy in PET-CT imaging and BMS Freedom to Discovery Grant.

References

1. Colby TV, Koss MN, Travis WD. Tumors of salivary gland type. Tumors of the lower respiratory tract: AFIP atlas of tumor pathology. 3rd series, Vol 13. Washington, DC: American Registry of Pathology; 1995. pp. 65–89.
2. Spencer H. Bronchial mucous gland tumours. Virchows Arch A Pathol Pathol Anat 1979;383:101–15.
3. Lack EE, Harris CBG, Erakllis AJ, Vawter GF. Primary bronchial tumors in childhood. A clinicopathologic study of six cases. Cancer 1983;51:492–7.
4. Yousem SA, Hochholzer L. Mucoepidermoid tumors of the lung. Cancer 1987;60:1346–52.
5. Klacsmann PG, Olson JL, Eggleston JC. Mucoepidermoid carcinoma of the bronchus: an electron microscopic study of the low grade and the high grade variants. Cancer 1979;43: 1720–33.
6. Kinoshita H, Shimotake T, Furukawa T, Deguchi E, Iwai N. Mucoepidermal carcinoma of the lung detected by positron emission tomography in a 5-year-old girl. J Pediatr Surg 2005;40:E1–3.
7. Yamada T, Chiba W, Yasuba H, Shimada T, Kudo M, Hamada K, et al. Successful treatment of bronchial mucoepidermoid carcinoma by bronchoplasty. Kyobu Geka 2005;58: 531–6.
8. Gould MK, Maclean CC, Kuschner WG, Rydzak CE, Owens DK. Accuracy of positron emission tomography for diagnosis of pulmonary nodules and mass lesions. A meta-analysis. JAMA 2001;285:914–24.
9. Marom EM, Sarvis S, Herndon JE 2nd, Patz EF Jr. T1 lung cancers: sensitivity of diagnosis with fluorodeoxyglucose PET. Radiology 2002;223:453–59.
10. Erasmus JJ, McAdams HP, Patz EF Jr, Coleman RE, Ahuja V, Goodman PC. Evaluation of primary pulmonary carcinoid tumors using FDG PET. AJR Am J Roentgenol. 1998;170: 1369–73.
11. Jadvar H, Segall GM. False-negative fluorine-18-FDG PET in metastatic carcinoid. J Nucl Med 1997;38:1382–3.
12. Ganim RB, Norton JA. Recent advances in carcinoid pathogenesis, diagnosis, and management. Surg Oncol 2000;9: 173–9.
13. Kruger S, Buck AK, Blumstein NM, Pauls S, Schelzig H, Kropf C, et al. Use of integrated FDG PET/CT imaging in pulmonary carcinoid tumours. J Intern Med 2006;260: 545–50.
14. Jain M, Yung E, Trow T, Katz DS. F-18 FDG positron emission tomography demonstration of pulmonary carcinoid. Clin Nucl Med 2004;29:370–1.
15. Wartski M, Alberini JL, Leroy-Ladurie F, Montpreville VD, Nguyen C, Corone C, et al. Typical and atypical bronchopulmonary carcinoid tumors on FDG PET/CT imaging. Clin Nucl Med 2004;29:752–3.
16. Daniels CE, Lowe VJ, Aubry MC, Allen MS, Jett JR. The utility of fluorodeoxyglucose positron emission tomography in the evaluation of carcinoid tumors presenting as pulmonary nodules. Chest 2007;131:255–60.

Epidermal growth factor receptor mutation status and clinicopathological features of combined small cell carcinoma with adenocarcinoma of the lung

Tomoya Fukui,[1,7] Koji Tsuta,[1] Koh Furuta,[2] Shun-ichi Watanabe,[3] Hisao Asamura,[3] Yuichiro Ohe,[4] Akiko Miyagi Maeshima,[5] Tatsuhiro Shibata,[6] Noriyuki Masuda[7] and Yoshihiro Matsuno[1,8]

[1]Clinical Laboratory Division, [2]Clinical Support Laboratory, [3]Thoracic Surgery Division, [4]Department of Medical Oncology, National Cancer Center Hospital, 5-1-1 Tsukiji, Chuo-ku, Tokyo 104-0045; [5]Pathology Division, [6]Cancer Genomics Project, National Cancer Center Research Institute, 5-1-1 Tsukiji, Chuo-ku, Tokyo 104-0045; [7]Department of Respiratory Disease, Graduate School of Medical Sciences, Kitasato University, 1-15-1 Kitasato, Sagamihara-shi, Kanagawa 228-8555, Japan

(Received June 4, 2007/Revised July 13, 2007/Accepted July 24, 2007/Online publication September 2, 2007)

In lung cancer, somatic mutations of epidermal growth factor receptor (*EGFR*) are concentrated in exons 18–21, especially in adenocarcinoma (Ad), but these mutations have rarely been reported in small cell lung carcinoma (SCLC). Combined SCLC is rare, and the *EGFR* mutation status and its relationship to the clinicopathological features of this tumor type have not yet been elucidated. We retrospectively studied six patients with combined SCLC with Ad components among 64 consecutive patients who underwent resection of SCLC. The clinicopathological features of each patient were reviewed, especially for the distribution pattern of the Ad component and lymph node metastases. *EGFR* mutations were screened by high-resolution melting analysis in each case, and were confirmed by sequencing of each mutation in the microdissected SCLC or Ad components. Regarding *EGFR*, no specific mutation was detected in five of the six patients, whereas one female patient who had never smoked had a missense mutation. In this case, both the SCLC and Ad components shared the same mutation in exon 21 (L858R). We identified a patient with combined SCLC with Ad sharing an identical *EGFR* mutation in both the SCLC and Ad components. In addition to the clinicopathological characteristics of this rare histological type of lung cancer, these findings provide useful information for better understanding the biology, natural history and clinical management of SCLC. (*Cancer Sci* 2007; 98: 1714–1719)

Small cell lung carcinoma (SCLC) accounts for 15–20% of all lung cancers worldwide.[1] SCLC is known to be more sensitive than non-SCLC to chemotherapy, but shows a more aggressive clinical course. The median survival time without treatment is 2–4 months.[2,3] Approximately 20% of patients with limited SCLC achieve a cure, but most patients with SCLC will relapse, and relapsed or refractory SCLC has a uniformly poor prognosis with a 5-year survival rate of less than 5%.[4]

According to the 2004 World Health Organization (WHO)/International Association for the Study of Lung Cancer (IASLC) classification of lung and pleural tumors,[5] 'combined SCLC' is defined as SCLC combined with an additional component that consists of any of the histological types of non-SCLC, usually adenocarcinoma (Ad), squamous cell carcinoma (Sq) or large cell carcinoma. Combined SCLC is rare, and has been reported to account for less than 1–3.2% of all SCLC.[6,7] However, a high proportion (12–26%) of SCLC patients who undergo surgical resection show combination with non-SCLC.[8–12]

In a clinical setting, the distinction of SCLC from non-SCLC is critical because of major differences in patient management and prognosis. Recently, molecular targeted therapy has been developed using agents such as epidermal growth factor receptor (EGFR) tyrosine kinase inhibitor, which exerts antitumor activity in patients with advanced non-SCLC (especially Ad) with *EGFR* mutations. High expression of EGFR has been reported in various epithelial malignant tumors, including lung cancer,[13,14] and somatic mutations in the kinase domain of *EGFR* are suggested to be strongly correlated with sensitivity to EGFR tyrosine kinase inhibitor.[15,16] These mutations are concentrated in exons 18–21 of *EGFR*, and approximately 90% of *EGFR*-mutant patients with lung Ad have mutations in two hot spots: in-frame deletion at codons 747–749 (DEL) in exon 19, and a missense mutation at codon 858 (L858R) in exon 21.[17,18] Although these mutations have rarely been reported in SCLC, two recent studies have demonstrated *EGFR* mutation in SCLC.[19,20]

In the present study, we retrospectively investigated six resected cases of combined SCLC with an Ad component to elucidate the clinicopathological features of this rare tumor, especially the ratio of each tumor component, the distribution patterns of the Ad component, and the status of lymph node metastasis. The *EGFR* mutation status in surgically resected specimens was also analyzed for each histological type in the same tumor.

Materials and Methods

Patients and histological diagnosis. A search of our surgical pathology files covering the period January 1982 to December 2004 yielded 64 consecutive patients with SCLC who had undergone surgical resection at the National Cancer Center Hospital, Tokyo, Japan. For the purposes of the present study, we identified six patients with combined SCLC with an Ad component. The research protocol was approved by the Institutional Review Board.

The surgically resected specimens were fixed in 10% formalin. All sections containing both tumor tissues and surrounding lung tissues were embedded in paraffin. Additional consecutive 5 μm-thick sections were cut from the tissue block and stained with hematoxylin and eosin. All histological diagnoses were reviewed by certificated pathologists (K. T., A. M. M. and Y. M.) based on the most recent WHO/IASLC classification of lung and pleural tumors.[5] Both clinical and pathological staging data for each patient have been reported according to the International Staging System for Lung Cancer.[21] Patient survival was calculated as the time between operation and death.

Immunohistochemistry and evaluation. For phenotypic analysis, paraffin section immunohistochemistry was carried out using the primary antibodies listed in Table 1, followed by subsequent labeling with the Envision+ horseradish peroxidase (HRP) system (DAKO, Carpinteria, CA, USA). For heat-induced epitope retrieval, sections stained for p63 were treated with 1.0 mmol/L

[8]To whom correspondence should be addressed.
E-mail: ymatsuno@med.hokudai.ac.jp

doi: 10.1111/j.1349-7006.2007.00600.x

Table 1. Results of immunohistochemistry

Patient no.	SCLC component (%)	Immunoreaction					Non-SCLC component (%)	Immunoreaction					No. tumor embolism cells per slice† (%)		
		CgA	SYN	NCAM	TTF-1	p63		CgA	SYN	NCAM	TTF-1	p63	SCLC	Ad	Sq
1	95	2+	3+	3+	3+	0	Ad, 5	1+	1+	1+	3+	0	30 (97)	1 (3)	–
2	80	3+	3+	3+	3+	0	Ad, 10	0	1+	1+	2+	1+	21 (84)	3 (12)	1 (4)
							Sq, 10	0	0	0	0	3+			
3	70	1+	3+	3+	3+	0	Ad, 30	0	1+	0	3+	0	38 (93)	3 (7)	–
4	55	2+	3+	3+	3+	0	Ad, 45	0	0	1+	1+	0	24 (92)	2 (8)	–
5	35	3+	3+	3+	3+	0	Ad, 60	1+	1+	1+	3+	1+	17 (100)	0 (0)	0 (0)
							Sq, 5	0	1+	0	0	2+			
6	5	Not done					Ad, 95	Not done					Not done		

CgA, chromogranin-A; NCAM, neural cell adhesion molecule; SCLC, small cell lung carcinoma; SYN, synaptophysin; TTF-1, thyroid transcription factor-1. Semiquantitative assessments of the percentage of positive tumor cells (0 = none, 1+ = 1–33%, 2+ = 34–66%, 3+ = 67–100%) were made. †We counted the number of lymph vessels with tumor embolisms confirmed by staining for D2-40 for a representative slide.

Table 2. Clinical characteristic of the patients with combined small cell lung carcinoma (SCLC) with adenocarcinoma (Ad)

Patient no.	Age/Sex	ECOG PS	Smoking status	Smoking index	Tumor location	Size (mm)	Stage (cTNM)	Preoperative diagnosis	Surgical procedure
1	74/Male	0	Current	2160	Peripheral	31	IIb (210)	Unknown	RLL†
2	66/Male	0	Ever	900	Peripheral	38	IIb (210)	Unknown	RM/LL‡
3	62/Female	0	Never	0	Peripheral	31	Ib (200)	SCLC	LUL
4	77/Male	1	Current	570	Peripheral	15	Ia (100)	Unknown	Left pneumonectomy
5	75/Male	0	Ever	1000	Peripheral	30	Ia (100)	Non-SCLC	RUL
6	76/Male	0	Current	1120	Peripheral	28	Ia (100)	Ad	RUL

Smoking index: (number of cigarettes smoked per day) × years. Adjuvant chemotherapy: †cyclosphosphamide + doxorubicin + vincristine × 1 cycle. ‡Cisplatin + etoposide × 1 cycle followed by cisplatin + irinotecan × 3 cycles. LUL, left upper lobectomy; RLL, right lower lobectomy; RM/LL, right middle and lower lobectomy; RUL, right upper lobectomy.

ethylenediaminetetraacetic acid buffer (pH 8.0). Sections stained for chromogranin A (1:500, polyclonal; DAKO), synaptophysin (1:100, polyclonal; DAKO), neural cell adhesion molecule (NCAM) (1:200, Lu243; Nihon Kayaku, Tokyo, Japan), thyroid transcription factor (TTF)-1 (1:100, 8G7G3/1; DAKO), p63 (1:100, 4A4; DAKO) and D2-40 (1:50, D2-40; DAKO) were treated with 0.02 mol/L citrate buffer (pH 6.0). The slides were incubated overnight with each primary antibody. Diaminobenzidine was used as the chromogen, and hematoxylin as the counterstain.

Positive staining was defined as distinct linear membrane staining for neural cell adhesion molecule, cytoplasmic staining for chromogranin A and synaptophysin, and nuclear staining for TTF-1 and p63. Immunostaining of each of the SCLC and non-SCLC components was graded on a scale of 0–3+ according to the percentage of positive tumor cells (0 = none; 1+ = 1–33%; 2+ = 34–66%; 3+ = 67–100%). We then carried out immunohistochemical identification of lymph vessels with or without tumor embolisms for a representative slide.[22] After independent evaluation by two of us (T. F. and K. T.), judgment consensus was obtained by joint viewing of the slides using a multiheaded microscope.

Analysis of *EGFR* mutational status. In our previous study, we established a practical and precise non-sequencing method for detecting *EGFR* mutations involving high-resolution melting analysis (HRMA) using LCGreen I dye (Idaho Technology, Salt Lake City, UT, USA).[23] First we screened for the *EGFR* mutations, DEL and L858R, using the HRMA method in formalin-fixed paraffin sections obtained from surgically resected combined SCLC with Ad. Human genomic DNA (Roche Diagnostics, Basel, Switzerland) was used as a control sample with wild-type *EGFR*. Second, we used 10% formalin-fixed, paraffin-embedded surgical specimens of primary combined SCLC from patients demonstrating DEL or L858R by HRMA, and the DNA was extracted from each of the SCLC and Ad components, respectively, the areas of which were clearly determined morphologically after laser capture microdissection (Arcturus Engineering, Mountain View, CA, USA) of the tumor tissue.[24] Nested polymerase chain reaction (PCR) was carried out to amplify exons 19 and 21 of *EGFR* using previously described primers.[17] The PCR products were electrophoresed on 2% agarose gels and subcloned into the TA vector (TOPO TA Cloning Kit, Invitrogen, Carlsbad, CA, USA), then the sequences were determined with M13 primers using an ABI Prism 3100 Genetic Analyzer (Applied Biosystems, Foster City, CA, USA) according to the manufacturer's instructions.

Results

Clinical characteristics. The clinical characteristics of the six patients are shown in Table 2. All patients were Japanese, aged between 62 and 77 years (mean 71.7 years). Five patients were male and one was female. Five patients were smokers whereas the remaining patient had never smoked. The median survival time of the six patients was 16.8 months (range 0.4–27.4 months); one patient died of heart failure 13 days after left pneumonectomy.

All six tumors were located in the peripheral portion of the lung. On clinical evaluation, three patients were staged as Ia (T1N0M0), one as Ib (T2N0M0) and two as IIb (T2N1M0). Preoperative pathological diagnoses were obtained in three patients and comprised one case each of SCLC, non-SCLC and Ad.

Pathological findings. Among six patients with combined SCLC with Ad, histological examination demonstrated that four had

Table 3. **Histological findings of primary tumor and lymph node metastases, and epidermal growth factor receptor (*EGFR*) mutation**

Patient no.	Stage (pTNM)	Ratio of each component (%)			Histological type of lymph node metastasis		BAC-like extension	*EGFR* mutation
		SCLC	Ad	Sq	Mediastinal	Hilar		
1	IIa (110)	95	5	0	Non†	SCLC	Absent	Wild type
2	IIIa (220)	80	10	10	SCLC	SCLC	Present	Wild type
3	IIIb (410)	70	30	0	Non†	Ad	Present	L858R
4	IIIb (420)	55	45	0	Ad	SCLC or Ad‡	Present	Wild type
5	IIIa (220)	35	60	5	Ad	SCLC or Ad‡	Present	Wild type
6	Ib (200)	5	95	0	Non†	Non†	Present	Wild type

†The patient had no mediastinal or hilar lymph node metastasis. ‡The patient had lymph node metastasis only from the SCLC component, and another lymph node showing metastasis only from the Ad component. Ad, adenocarcinoma; BAC, bronchioloalveolar carcinoma; hilar, hilar lymph node; L858R, mutation at codon 858 of *EGFR*; medical, mediastinum lymph node; pTNM, pathological TNM; SCLC, small cell lung carcinoma; Sq, squamous cell carcinoma.

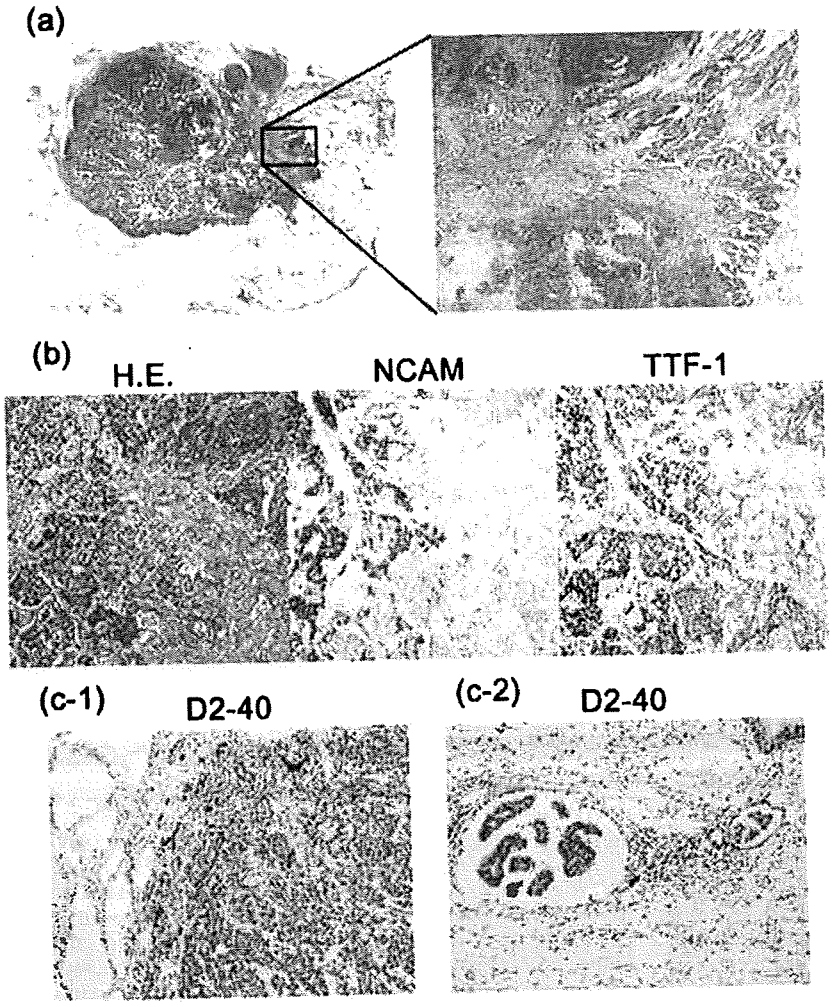

Fig. 1. Combined small cell lung carcinoma (SCLC) with adenocarcinoma (Ad). (a) The periphery of this tumor consisted of a non-mucinous bronchioloalveolar carcinoma-like extension (patient no. 3). (b) The transitional zone between the SCLC and Ad components had poorly differentiated cells, shown by the immunohistochemical studies (patient no. 1). (c) D2-40 with a membranous staining pattern of the lymph vessels. Tumor embolism of lymph vessels was confirmed by D2-40 staining (patient no. 3). (c-1) SCLC cell embolisms increased in number around the primary lesion. (c-2) Ad cell embolisms invaded the lymph vessels.

SCLC combined only with an Ad component (ratio of Ad in the tumor: 5, 30, 45 and 95%), whereas two had both Ad and Sq components (ratio of Ad/Sq: 10%/10% and 60%/5%, respectively). On pathological staging, one patient was staged as Ib (T2N0M0), one as IIa (T1N1M0), two as IIIa (T2N2M0) and two as IIIb (T4N1M0 and T4N2M0). In five of the six patients, the Ad components were observed in the peripheral part of the tumor showing a lepidic extension pattern, simulating bronchioloalveolar carcinoma. In the remaining one patient, Ad formed a minor component comprising approximately 5% of the tumor (Table 3). The Ad components in two patients showed a micropapillary growth pattern, whereas mucin production was not detected in any patient (Fig. 1a). The boundary between the SCLC and Ad components was not clear, and showed an

doi: 10.1111/j.1349-7006.2007.00600.x

indeterminate component that suggested gradual morphological transition from one to the other (Fig. 1b). In the two patients who also had combined Sq, the Sq component showed keratinization and was distinct from the SCLC component, but the border between the Ad and Sq components was unclear.

The results of immunohistochemical studies carried out in five cases are shown in Table 1. The specimen from patient no. 6 was not available. All of the SCLC components showed positive staining for at least one neuroendocrine marker. In addition, the Ad components in all five patients examined showed positive staining for at least one neuroendocrine marker, although semiquantitative assessments of the percentage of positive Ad cells were lower than those for SCLC cells in the same tumor. Also, the Ad components showed positive staining for TTF-1 in all five patients. TTF-1 staining of the SCLC component tended to be similar to that of the Ad component in terms of the percentage of positive cells. p63 immunostaining served as a good marker of Sq differentiation.

Status of lymph node metastasis. Five patients had pathologically confirmed hilar lymph node metastases, and three of them also had histologically proven mediastinal lymph node metastases, which had not been evident at the time of preoperative clinical evaluation (Table 3). Among these five patients with hilar lymph node metastases, two showed only SCLC in the metastatic lesion, one showed Ad only, and two showed SCLC or an Ad component that had developed separately in each lymph node. Among the three patients with mediastinal lymph node metastases, one had only SCLC in the nodes, and two had an Ad component only. Metastatic Ad components were found only in patients with a primary tumor in which Ad accounted for more than 30% of the total volume.

In the six patients, we identified tumor embolism of the lymph vessels immunohistochemically with D2-40 staining. There were approximately 800–1000 lymph vessels in each of these tumors per representative slide. The major component invading the lymph vessels around the tumors was SCLC cells. Even in the two patients who had mediastinal lymph node metastases with an Ad component, the SCLC cells tended to spread to the lymph vessels rather than the Ad cells (Table 1).

***EGFR* mutational status.** First, we analyzed 10 surgically resected samples from six patients with combined SCLC and Ad by HRMA. Analysis of exon 19 demonstrated curves identical to those of the control (wild type) in all samples, as shown in Fig. 2a. In the analysis of exon 21, thorough melting curves were obtained for two samples from patient no. 3, showing a different curve from the control, whereas the other eight samples demonstrated curves identical to the control (wild type), as shown in Fig. 2b. The normal lung tissue from patient no. 3, who was a female non-smoker, showed a wild-type curve, and therefore we judged that this patient had L858R in exon 21 of *EGFR*.

Next we confirmed this mutation in the SCLC and Ad components in patient no. 3. DNA was extracted from each SCLC and Ad component separately using laser capture microdissection or by manual microdissection, which was carried out for each clearly determined component on paraffin-embedded sections. Sequence analysis of subcloned PCR products obtained from the separate components was carried out. Examination of both SCLC and Ad components showed an identical mutation (L858R) in exon 21 (Fig. 3), confirming the results obtained by HRMA.

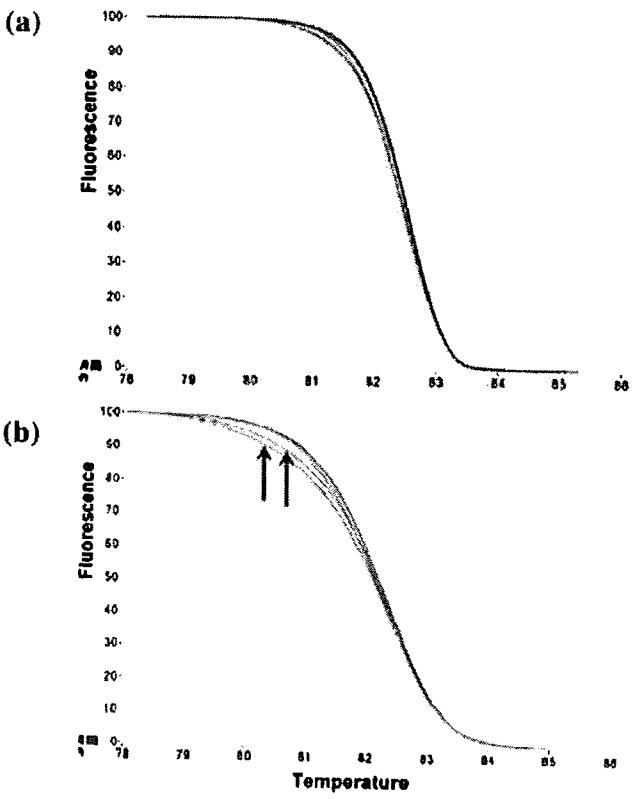

Fig. 2. Results of high-resolution melting analysis (HRMA). Adjusted melting curves obtained by HRMA of combined small cell lung carcinoma (SCLC) with primers designed to detect mutations in (a) exon 19 or (b) exon 21 of epidermal growth factor receptor (*EGFR*). Two samples from patient no. 3 were identified as containing the L858R mutations (↑). The DNA extracted from normal lung tissue of patient no. 3 was identified as wild type (not shown).

Discussion

The present study using microdissected tumor tissue is the first to report a patient with combined SCLC with Ad showing the *EGFR* mutation in both the SCLC and Ad components. *EGFR* mutations, especially DEL and L858R, have been reported in Ad of the lung. These somatic mutations in the kinase domain of *EGFR* have been shown to be predictive molecular markers for sensitivity to kinase inhibitors such as gefitinib (Iressa; AstraZeneca, Osaka, Japan). However, these mutations have rarely been demonstrated in SCLC. To our knowledge, there have been two reported cases of metastatic SCLC harboring DEL in exon 19 of *EGFR* showing responsiveness to EGFR tyrosine kinase inhibitors.[19,20,25] Considering that the diagnosis of SCLC is often based on small biopsy specimens that may not be sufficiently representative of the total tumor, there is a possibility that any combined component may be overlooked.

In a clinical setting, the distinction of SCLC from non-SCLC is critical because of major differences in management and prognosis between the two cancers. SCLC is well known to be more common in men and smokers, but so far SCLC with *EGFR* mutations has been detected only in female patients who have never smoked,[19,20] as was the case in our present female patient. Thus it seems reasonable to suggest that in clinically unusual SCLC patients, for example those who are non-smokers and female, showing peripheral nodular lesions and histological combination with Ad, *EGFR* mutation status should be analyzed because previous studies have shown that EGFR tyrosine kinase inhibitors are effective in patients with metastatic SCLC with *EGFR* mutations.

The present study is considerably informative with regard to the origin and histogenesis of SCLC. *EGFR* mutation is detected in patients with pre-invasive adenocarcinomatous lesions such as atypical adenomatous hyperplasia and bronchioloalveolar

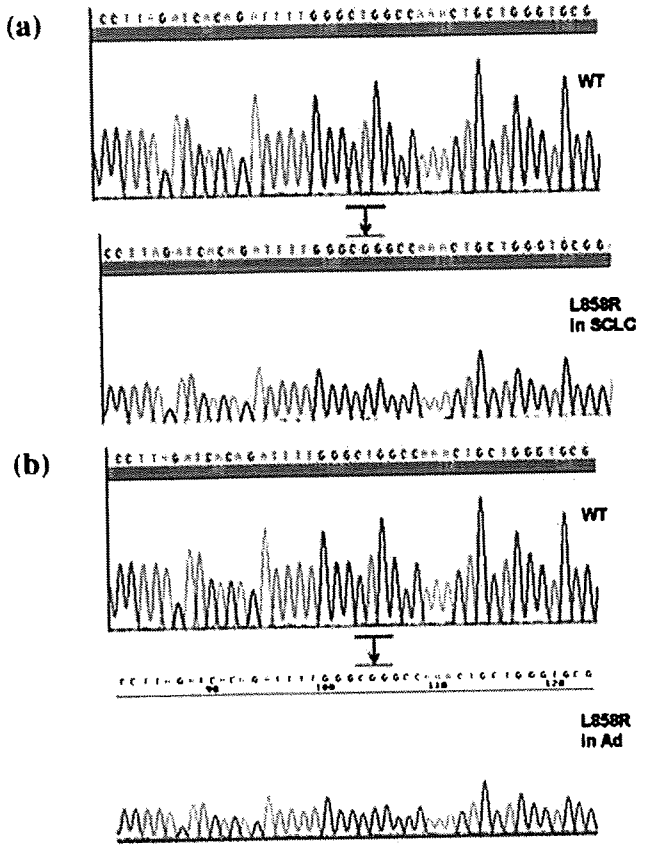

Fig. 3. Results of DNA sequencing from patient no. 3. The tumor of patient no. 3 was microdissected into the small cell lung carcinoma (SCLC) and adenocarcinoma (Ad) components. (a) Sequence analysis of the subcloned polymerase chain reaction (PCR) products from the microdissected SCLC component. (b) Sequence analysis of the subcloned PCR products from the microdissected Ad component. The patient had a tumor with L858R of EGFR, which was in both the SCLC and Ad components.

carcinoma, which eventually progress to invasive lung Ad.[26] In addition, *EGFR* mutations are also linked to Ad with a bronchioloalveolar carcinoma component.[27] Thus it is suggested that *EGFR* mutation occurs and plays a critical role in the early developmental stage of lung Ad. The mutation is detected more frequently in Ad in female non-smokers than in male smokers. In the present study, the only patient with SCLC harboring an *EGFR* mutation was female and a non-smoker, and the combined Ad component also harbored the same mutation. Moreover, as mentioned above, the two SCLC patients with *EGFR* mutation reported previously were also female and non-smokers. These findings imply that the mutations are an early genetic event in carcinogenesis of the lung and at least a certain proportion of SCLC may originate as a result of progression or transformation of Ad harboring *EGFR* mutation.

This phenomenon can also be linked to pathological features. The histological patterns of lymph node involvement showed that Ad components spread to mediastinal lymph nodes in the patients with hilar lymph node involved by SCLC or Ad component. Considering the status of tumor embolism of the lymph vessels observed using D2-40 staining, SCLC cell embolisms, but not Ad, increase in number around primary lesion in these tumors. It is suggested that a common uncommitted stem cell might differentiate into each component after involvement in a lymph node. Furthermore, positive staining for TTF-1, which is a highly specific immunohistochemical marker identifying carcinomas of pulmonary origin (especially non-mucinous Ad and SCLC),[28] was shown in the SCLC and Ad components, but not Sq. Previous studies have demonstrated TTF-1 expression in 83–100% of SCLC, but low expression in Sq.[29,30] These findings could be interpreted as being compatible with the hypothesis that SCLC and Ad originate from a common uncommitted stem (or precursor) cell originally expressing TTF-1.[31] It is possible to postulate that a fraction of SCLC possessing stem (or precursor) cell properties might have the potential to form an Ad component. In fact, in the present cases, there were some areas comprising morphologically indeterminate tumor cell components at the border of the SCLC and Ad components.

The rarity of patients with combined SCLC makes it difficult to determine the optimal management and biological characteristics of this tumor. However, the present findings suggest that the classical classification of lung cancer might provide insufficient management for a specified subpopulation in molecular targeted therapy. Although this retrospective study examined only a very limited number of lung carcinoma cases, we consider that the findings provide useful information for understanding the biology of this lung cancer and devising more effective forms of clinical management.

Acknowledgments

This study was supported in part by a Grant-in-Aid for Young Scientists from the Ministry of Education, Culture, Sports, Science and Technology, and for the Comprehensive 10-Year Strategy for Cancer Control from the Ministry of Health, Labor and Welfare, Japan and the Program for Promotion of Fundamental Studies in Health Sciences of the National Institute of Biomedical Innovation, Japan. We thank Karin Yokozawa and Kiyoaki Nomoto for their technical support.

References

1 Stupp R, Monnerat C, Turrisi AT 3rd, Perry MC, Leyvraz S. Small cell lung cancer: state of the art and feature perspectives. *Lung Cancer* 2004; **45**: 105–17.
2 Chua YJ, Steer C, Yip D. Recent advances in management of small-cell lung cancer. *Cancer Treat Rev* 2004; **30**: 521–43.
3 Aisner J. Extensive-disease small-cell lung cancer: the thrill of victory, the agony of defeat. *J Clin Oncol* 1996; **14**: 658–65.
4 Simon GR, Wagner H. Small cell lung cancer. *Chest* 2003; **123**: 259S–71S.
5 Travis WD, Coby TV, Corrin B, Shimosato Y, Brambilla E. *World Health Organization International Histological Classification of Tumours; Histological Typing of Lung and Pleural Tumours*, 3rd edn. Berlin: Springer, 1999.
6 Fraire AE, Johnson EH, Yesner R, Zhang XB, Spjut HJ, Greenberg SD. Prognostic significance of histopathologic subtype and stage in small cell lung cancer. *Hum Pathol* 1992; **23**: 520–8.
7 Mangum MD, Greco FA, Hainsworth JD, Hande KR, Johnson DH. Combined small-cell and non-small-cell lung cancer. *J Clin Oncol* 1989; **7**: 607–12.
8 Hage R, Elbers JR, Brutel de la Riviere A, van den Bosch JM. Surgery for combined type small cell lung carcinoma. *Thorax* 1998; **53**: 450–3.
9 Nicholson SA, Beasley MB, Brambilla E *et al.* Small cell lung carcinoma (SCLC): a clinicopathologic study of 100 cases with surgical specimens. *Am J Surg Pathol* 2002; **26**: 1184–97.
10 Lucchi M, Mussi A, Chella A *et al.* Surgery in the management of small cell lung cancer. *Eur J Cardiothorac Surg* 1997; **12**: 689–93.
11 de Antonio DG, Alfageme F, Gamez P, Cordoba M, Varela A. Results of surgery in small cell carcinoma of the lung. *Lung Cancer* 2006; **52**: 299–304.
12 Deslauriers J. Surgery for small cell lung cancer. *Lung Cancer* 1997; **17**: S91–8.
13 Ozanne B, Richards CS, Hendler F, Burns D, Gusterson B. Over-expression of the EGF receptor is a hallmark of squamous cell carcinomas. *J Pathol* 1986; **149**: 9–14.
14 Cerny T, Barnes DM, Hasleton P *et al.* Expression of epidermal growth factor receptor (EGF-R) in human lung tumours. *Br J Cancer* 1986; **54**: 265–9.

doi: 10.1111/j.1349-7006.2007.00600.x

15 Lynch TJ, Bell DW, Sordella R *et al.* Activating mutations in the epidermal growth factor receptor underlying responsiveness of non-small-cell lung cancer to gefitinib. *N Engl J Med* 2004; **350**: 2129–39.
16 Paez JG, Janne PA, Lee JC *et al.* EGFR mutations in lung cancer: correlation with clinical response to gefitinib therapy. *Science* 2004; **304**: 1497–500.
17 Takano T, Ohe Y, Sakamoto H *et al.* Epidermal growth factor receptor gene mutations and increased copy numbers predict gefitinib sensitivity in patients with recurrent non-small-cell lung cancer. *J Clin Oncol* 2005; **23**: 6829–37.
18 Pao W, Miller VA. Epidermal growth factor receptor mutations, small-molecule kinase inhibitors, and non-small-cell lung cancer: current knowledge and future directions. *J Clin Oncol* 2005; **23**: 2556–68.
19 Okamoto I, Araki J, Suto R, Shimada M, Nakagawa K, Fukuoka M. EGFR mutation in gefitinib-responsive small-cell lung cancer. *Ann Oncol* 2005; **17**: 1028–9.
20 Zakowski MF, Ladanyi M, Kris MG. EGFR mutations in small-cell lung cancers in patients who have never smoked. *N Engl J Med* 2006; **355**: 213–15.
21 Mountain CF. Revisions in the international system for staging lung cancer. *Chest* 1997; **111**: 1710–17.
22 Evangelou E, Kyzas PA, Trikalinos TA. Comparison of the diagnostic accuracy of lymphatic endothelium markers: Bayesian approach. *Mod Pathol* 2005; **18**: 1490–7.
23 Nomoto K, Tsuta K, Takano T *et al.* Detection of EGFR mutations in archived cytologic specimens of non-small cell lung cancer using high-resolution melting analysis. *Am J Clin Pathol* 2006; **126**: 608–15.
24 Emmert-Buck MR, Bonner RF, Smith PD *et al.* Laser capture microdissection. *Science* 1996; **274**: 998–1001.
25 Araki J, Okamoto I, Suto R, Ichikawa Y, Sasaki J. Efficacy of the tyrosine kinase inhibitor gefitinib in a patient with metastatic small cell lung cancer. *Lung Cancer* 2005; **48**: 141–4.
26 Yoshida Y, Shibata T, Kokubu A *et al.* Mutations of the epidermal growth factor receptor gene in atypical adenomatous hyperplasia and bronchioloalveolar carcinoma of the lung. *Lung Cancer* 2005; **50**: 1–8.
27 Blons H, Cote JF, Le Corre D *et al.* Epidermal growth factor receptor mutation in lung cancer are linked to bronchioloalveolar differentiation. *Am J Surg Pathol* 2006; **30**: 1309–15.
28 Stahlman MT, Gray ME, Whitsett JA. Expression of thyroid transcription factor-1 (TTF-1) in fetal and neonatal human lung. *J Histochem Cytochem* 1996; **44**: 673–8.
29 Jerome Marson V, Mazieres J, Groussard O *et al.* Expression of TTF-1 and cytokeratins in primary and secondary epithelial lung tumours: correlation with histological type and grade. *Histopathology* 2004; **45**: 125–34.
30. Kalhor N, Zander DS, Liu J. TTF-1 and p63 for distinguishing pulmonary small-cell carcinoma from poorly differentiated squamous cell carcinoma in previously pap-stained cytologic material. *Mod Pathol* 2006; **19**: 1117–23.
31 Sturm N, Lantuejoul S, Laverriere MH *et al.* Thyroid transcription factor 1 and cytokeratins 1, 5, 10, 14 (34βE12) expression in basaloid and large-cell neuroendocrine carcinomas of the lung. *Hum Pathol* 2001; **32**: 918–25.

Modern Pathology (2007) 20, 215–220
 0893-3952/07 $30.00
www.modernpathology.org

Immunohistochemical detection of GLUT-1 can discriminate between reactive mesothelium and malignant mesothelioma

Yasufumi Kato[1,2], Koji Tsuta[1], Kunihiko Seki[1], Akiko Miyagi Maeshima[3], Shunichi Watanabe[2], Kenji Suzuki[2], Hisao Asamura[2], Ryosuke Tsuchiya[2] and Yoshihiro Matsuno[1]

[1]*Clinical Laboratory, National Cancer Center Hospital, Tokyo, Japan;* [2]*Thoracic Surgery Divisions, National Cancer Center Hospital, Tokyo, Japan and* [3]*Pathology Division, National Cancer Center Research Institute, Tokyo, Japan*

The separation of benign reactive mesothelium (RM) from malignant mesothelial proliferation can be a major challenge. A number of markers have been proposed, including epithelial membrane antigen, p53 protein, and P-glycoprotein. To date, however, no immunohistochemical marker that allows unequivocal discrimination of RM from malignant pleural mesothelioma (MPM) has been available. A family of glucose transporter isoforms (GLUT), of which GLUT-1 is a member, facilitate the entry of glucose into cells. GLUT-1 is largely undetectable by immunohistochemistry in normal epithelial tissues and benign tumors, but is expressed in a variety of malignancies. Thus, the expression of GLUT-1 appears to be a potential marker of malignant transformation. Recently, in fact, some studies have shown that GLUT-1 expression is useful for distinguishing benign from malignant lesions. The purpose of the present study was to evaluate the diagnostic utility of GLUT-1 expression for diagnostic differentiation between RM and MPM. Immunohistochemical staining for GLUT-1 was performed in 40 cases of RM, 48 cases of MPM, and 58 cases of lung carcinoma. Immunohistochemical GLUT-1 expression was seen in 40 of 40 (100%) MPMs, and in all cases the expression was demonstrated by linear plasma membrane staining, sometimes with cytoplasmic staining in addition. GLUT-1 expression was also observed in 56 out of 58 (96.5%) lung carcinomas. On the other hand, no RM cases were positive for GLUT-1. GLUT-1 is a sensitive and specific immunohistochemical marker enabling differential diagnosis of RM from MPM, whereas it cannot discriminate MPM from lung carcinoma.
Modern Pathology (2007) **20**, 215–220. doi:10.1038/modpathol.3800732; published online 22 December 2006

Keywords: Glut-1; reactive methothelium; malignant pleural mesothelioma; immunohistochemistry; lung carcinoma

The separation of benign reactive mesothelium (RM) from malignant mesothelial proliferation can be a major challenge. The common cytomorphological features associated with malignancy, such as high cellularity/proliferation, marked cytonuclear atypia and high mitotic rate are of very limited use in this setting. Thus, it is sometimes very difficult, or almost impossible even for expert pathologists to make a definite diagnosis of malignant mesothelioma, especially in small specimens, unless there is unequivocal invasion of adjacent tissues by tumor cells.[1] On the other hand, early diagnosis of malignant pleural mesothelioma (MPM) in small closed pleural biopsy samples, or by cytology, is crucial for patient management and may facilitate the avoidance of invasive surgical procedures.

A number of immunohistochemical markers have been proposed to assist conventional morphological diagnosis, including epithelial membrane antigen (EMA)[2–5] p53 protein,[2–11] and P-glycoprotein.[2,5,12] Other markers tested have included Bcl-2,[2,3,13] platelet-derived growth factor receptor (PDGF-R) β-chain[2,5,6] and desmin.[2] To date, however, no single immunohistochemical marker that can unequivocally discriminate RM from MPM has been available.

GLUT-1 is one of 14 members of the mammalian facilitative glucose transporter (GLUT) family of passive carriers that function as an energy-independent system for transport of glucose down a concentration gradient.[14] GLUT-1 is not detectable

Correspondence: Dr Y Matsuno, MD, Clinical Laboratory Division, National Cancer Center Hospital, 1-1, Tsukiji 5-chome, Chuo-ku, Tokyo 104-0045, Japan.
E-mail: ymatsuno@ncc.go.jp
Received 30 August 2006; accepted 23 October 2006; published online 22 December 2006

in a large proportion of cells from normal tissues and benign lesions, except for erythrocytes, germinal cells of the testis, renal tubules, perineurium of peripheral nerves, endothelial cells in blood–brain barrier vessels, and placenta (trophoblasts and capillaries).[15,16] In contrast, GLUT-1 is expressed in a variety of carcinomas such as those of the breast, head and neck, bladder, renal cells, and lung.[15–24] Previous reports suggest that the expression of GLUT-1 may be a potential marker for malignancy.

Recently, some studies have shown that GLUT-1 expression is useful for resolving the common diagnostic dilemma of distinguishing benign from malignant lesions.[25,26] Although a few studies have demonstrated that GLUT-1 is useful for distinguishing RM from metastatic adenocarcinoma in body cavity effusions,[27–29] the study cohorts did not include MPM. Using immunohistochemistry, Godoy *et al*[16] analyzed coexpression of GLUT-1 and other GLUT isoforms (GLUT-2 to -6 and GLUT-9) in a variety of benign and malignant tumors, and demonstrated that two of four MPMs were positive for GLUT-1. However, they did not analyze reactive and normal mesothelium.

The purpose of the present study was to evaluate the diagnostic utility of GLUT-1 detection for differential diagnosis between RM and MPM.

Materials and methods

Case Selection

The materials for the present study were extracted from cases deposited in the pathology files of the National Cancer Center Hospital, Tokyo, between 1971 and 2005. They comprised 40 cases of RM, 48 cases of MPM (epithelioid, 36 cases; biphasic, 11 cases; sarcomatoid, 1 case), and 58 cases of lung carcinoma (squamous cell carcinoma, 28 cases; adenocarcinoma, 30 cases). All diagnoses had been made on the basis of conventional histopathologic features evident in slide preparations stained with hematoxylin and eosin, some special stains, and immunohistochemical techniques available at that time.[30,31] In the present study, immunohistochemistry for D2-40 and calretinin was added for all cases to confirm the identity of mesothelial cells (see below).

Immunohistochemistry

For immunohistochemical staining, 5-μm-thick sections were deparaffinized and treated with 3% hydrogen peroxide for 30 min to block endogenous peroxidase activity, followed by washing in deionized water for 2–3 min. Heat-induced epitope retrieval with Target Retrieval Solution (DAKO, Carpinteria, CA, USA) was performed for GLUT-1 and calretinin. After the slides had been allowed to cool at room temperature for 40 min, they were rinsed with deionized water and then washed in phosphate-buffered saline for 5 min. The slides were then stained by overnight incubation with primary antibodies against GLUT-1 (1:200, polyclonal, Dako), D2-40 (1:200, clone D2-40, Signet Laboratories, Dedham, MA, USA), and calretinin (1:100, polyclonal, Zymed, San Francisco, CA, USA). Immunoreactions were detected by the labeled streptavidin–biotin method, and visualized with 3, 3′-diaminobenzidine, followed by counterstaining with hematoxylin. Appropriate positive and negative controls (red blood cells for GLUT-1) were used for each antibody. The area of GLUT-1 staining was evaluated on a sliding scale of 0 to 3+ to represent the percentage of positive cells among mesothelial cells (indicated by D2-40 and calretinin immunostain) or tumor cells (0 = <1%, 1+ = 1–25%, 2+ = 26–50%, 3+ = >51%). Immunohistochemical staining was scored independently by two observers (YK and KT).

Results

The results of immunohistochemistry are summarized in Table 1. GLUT-1 expression was demonstrated by distinct linear plasma membrane staining, sometimes with cytoplasmic staining in addition

Table 1 Immunoreactivity of GLUT-1

	n	*GLUT-1 positive (%)*	*Staining area*			
			0	*1+*	*2+*	*3+*
Mesothelioma, all subtypes	48	48 (100)	0	15	15	18
Epithelioid	36	36 (100)	0	9	12	15
Biphasic	11	10 (90.9)[a] 7 (63.6)[b]	1[a] 4[b]	6[a] 3[b]	3[a] 2[b]	1[a] 2[b]
Sarcomatoid	1	1 (100)	0	1	0	0
Reactive mesothelium	40	0 (0)	40	0	0	0
Lung carcinoma	58	56 (96.5)	2	12	9	35
Squamous cell carcinoma	28	28 (100)	0	1	3	24
Adenocarcinoma	30	28 (93.3)	2	11	6	11

[a]Epithelioid areas.

[b]Sarcomatoid areas.

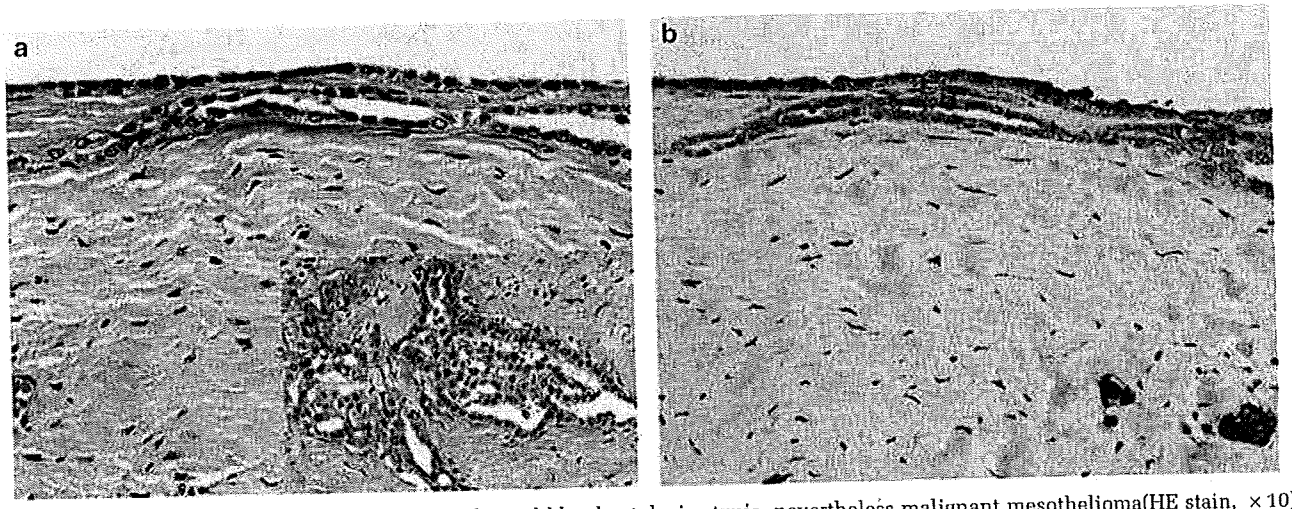

Figure 1 (a) In the surface area, the tumor cells showed bland cytologic atypia, nevertheless malignant mesothelioma(HE stain, ×10). Inset: the tumor cells arranged complex branching tubular formation (HE stain, ×10). (b) Most of the tumor cells in the epithelioid MPM were positive for GLUT-1 and red blood cells were served as internal positive control (×10).

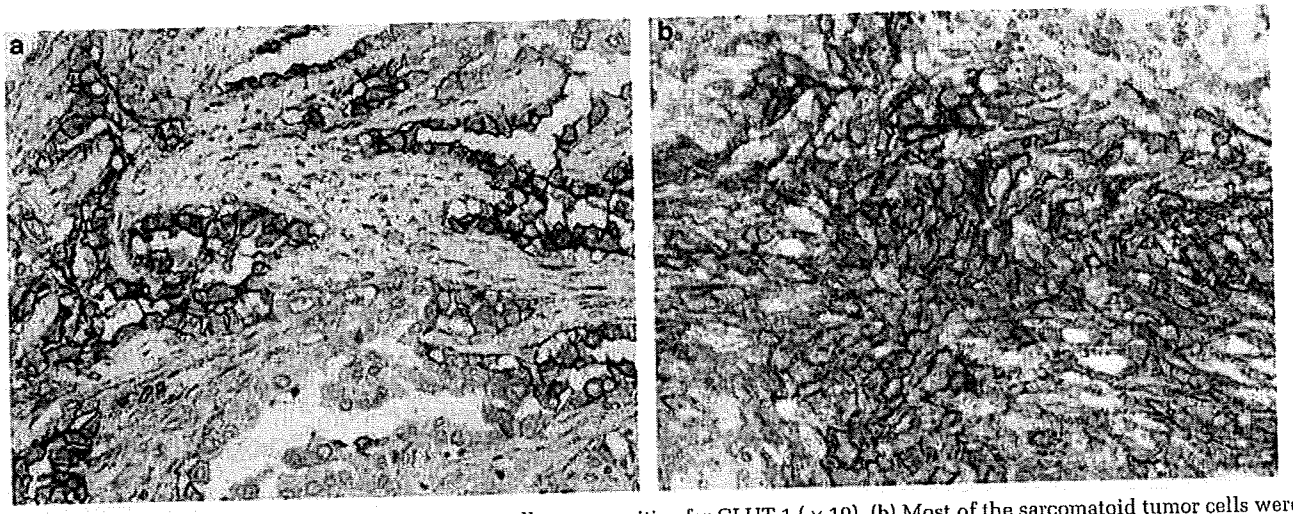

Figure 2 (a) More than half of the epithelioid tumor cells were positive for GLUT-1 (×10). (b) Most of the sarcomatoid tumor cells were positive for GLUT-1 (×10). The immunoreactivity was observed as distinct linear plasma membrane staining, with weak cytoplasmic staining in addition.

Table 2 GLUT-1 immunoreactivity acording to MPM histological subtype

	n	*GLUT-1-positive (%)*	*Staining area*			
			0	*1+*	*2+*	*3+*
Epithelioid area	47	46 (97.8)	1	15	15	16
Sarcomatoid area	12	8 (66.7)	4	4	2	2

(Figure 1a and b). GLUT-1 immunoreactivity was seen in 48 of 48 (100%) MPM cases, whereas no RM cases were positive for GLUT-1.

We also evaluated GLUT-1 immunoreactivity according to histological subtype, as shown in Table 2. Immunoreactivity was observed in 46 of 47 (96.7%) epithelioid mesothelioma (Figure 2a) including epithelioid areas of biphasic mesothelioma, and in seven of 12 (66.7%) sarcomatoid mesothelioma (Figure 2b) including sarcomatoid areas of biphasic mesothelioma. However, immunoreactive cells more than half of tumor cell was only 16 of 47 (34%) of epithelioid mesothelioma including epithelioid areas of biphasic mesothelioma, and two of 12 (14.1%) of sarcomatoid mesothelioma including sarcomatoid areas of biphasic mesothelioma. The GLUT-1-positive cells varied from a few cells to almost all cells in the clusters, but no characteristic staining pattern was observed in MPM.

GLUT-1 immunoreactivity was also seen in 56 of 58 (96.5%) cases of lung carcinoma. According to histological subtype, immunoreactivity was

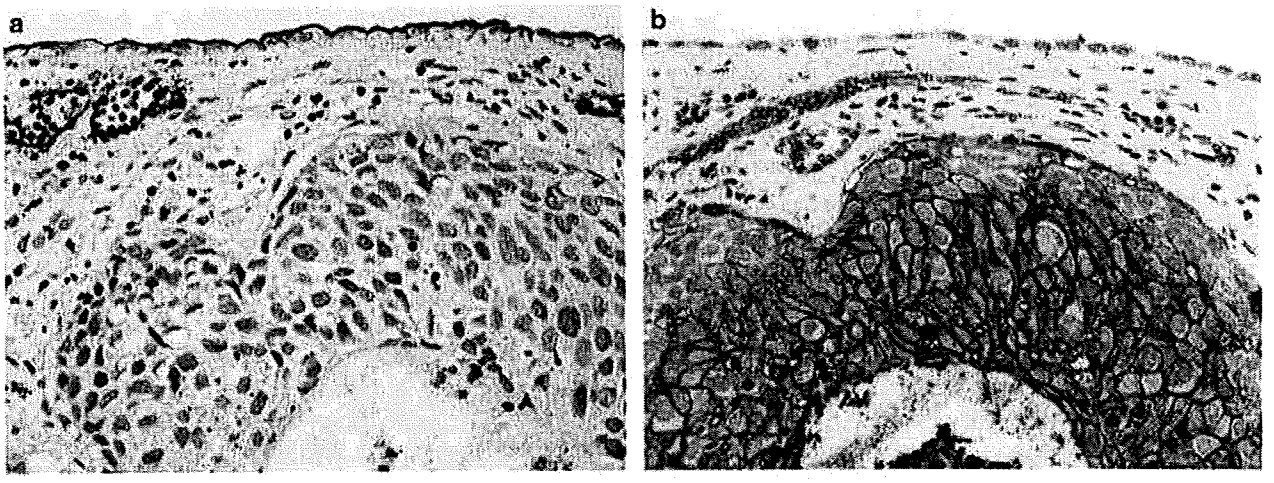

Figure 3 (a) D2-40 immunoreactivity was observed in the RM and lymph vessels beneath the pleura, but no immunoreactivity was observed in the poorly differentiated squamous cell carcinoma (× 10). (b) Most of the tumor cells without peripheral lesion in of the poorly differentiated squamous cell carcinoma were positive for GLUT-1 (red blood cells were served as internal positive control). On the other hand, RM showed no immunoreactivity for GLUT-1 (× 10).

observed in 28 of 28 (100%) cases of squamous cell carcinoma (Figure 3a and b) and 28 of 30 (93.3%) cases of adenocarcinoma. In squamous cell carcinoma, the area of positive staining was 3+ in 24 of 28 (85.7%) cases, compared with only 11 of 30 (36.7%) in cases of adenocarcinoma. Also in squamous cell carcinoma, a characteristic staining pattern was observed; tumor cells showed more intensely positive staining in the central area of tumor nests than in the peripheral area (Figure 3b).

Discussion

Morphologic differentiation between RM and MPM in small specimens can be a diagnostic challenge. The difficulty is compounded when neoplastic cells demonstrate only slight atypia. In addition, there are currently no reliable markers that allow immunohistochemical discrimination between RM and MPM. In the present study, we clearly demonstrated that GLUT-1 is a sensitive and specific immunohistochemical marker that can differentiate RM from MPM. To our knowledge, this is the first report to describe the usefulness of GLUT-1 immunostaining for discriminating between RM and MPM.

Elevated levels of expression or activation of GLUT-1, or both, have been shown to be associated with transformation of cells and malignancy, and to be modified by changes in the physiological microenvironment in tissues.[32,33] High GLUT-1 expression correlates with increased metabolism and glucose utilization in a number of normal tissues, and this transporter is overexpressed in a variety of human tumors.[15,16] Increased expression of GLUT-1 is also seen in conditions that induce greater dependency on glycolysis as an energy source, such as ischemia, hypoxia, or both.[34] These data suggest that overexpression of GLUT-1 may play an important role in the survival of tumor cells by maintaining an adequate energy supply to support their high metabolism and rapid growth in an often less-than-ideal physiological environment.[35]

GLUT-1 expression has been revealed in a variety of carcinomas, such as those of the breast, head and neck, bladder, and renal cells.[15–19,23] In the lung, about 34.3–100% of lung adenocarcinomas[16,20–22,24] and 100% of lung squamous cell carcinomas[20–22,24] are reported to express GLUT-1 at the primary site. With regard to MPM, only one article has describe that two of four studied cases were positive for GLUT-1.[16] In the present study, GLUT-1 immunoreactivity was observed in all MPMs and 56 out of 58 (96.5%) cases of lung carcinoma. These results indicate that GLUT-1 cannot discriminate between MPM and lung carcinoma. Therefore, additional appropriate positive and negative mesothelial markers are needed in order to differentiate between MPM and lung carcinoma.[31]

The heterogeneity of GLUT-1-positive areas has been reported previously. In squamous cell carcinoma, cells in the center of cancer nests, close to the necrotic area, were stained more strongly than those in peripheral areas. In adenocarcinoma, poorly differentiated areas such as the solid central area were stained more strongly than well differentiated areas such as those showing lepidic growth.[20–22,24] In the present study, more than half of all tumor cells were positive for GLUT-1 in 37.5% of MPMs, 85.7% of lung squamous cell carcinomas, and 36.7% of lung adenocarcinomas. These results indicate that GLUT-1 negativity in small samples such as those obtained by biopsy does not exclude malignancy, and that positive immunoreactivity for GLUT-1 may be an aid to accurate diagnosis of malignancy.

The GLUT-1 positivity rate in RM has been reported to be 0% (present study and Afify *et al*[29]), 3% (Zimmerman *et al*[28]), and 20% (Burstein *et al*[27]).